RSC Advances

PAPER

View Article Online
View Journal | View Issue

Cite this: RSC Adv., 2015, 5, 12879

An alkylthieno-2-yl flanked dithieno[2,3-*d*:2′,3′-*d*′]-benzo[1,2-*b*:4,5-*b*′]dithiophene-based low band gap conjugated polymer for high performance photovoltaic solar cells†

Pengzhi Guo,[a] Yangjun Xia,*[a] Fei Huang,*[b] Guoping Luo,[b] Jianfeng Li,[a] Peng Zhang,[a] Yuancheng Zhu,[c] Chunyan Yang,[a] Hongbin Wu[b] and Yong Cao[b]

Received 14th November 2014
Accepted 15th January 2015

DOI: 10.1039/c4ra14532a

www.rsc.org/advances

A low band gap conjugated polymer derived from alkylthieno-2-yl flanked dithieno[2,3-*d*:2′,3′-*d*′]benzo[1,2-*b*:4,5-*b*′]dithiophene and a naphtho[1,2-*c*:5,6-*c*]bis[1,2,5]thiadiazole derivative was first synthesized, and high performance inverted photovoltaic solar cells with a power conversion efficiency of 7.52% have been demonstrated.

Introduction

Bulk heterojunction polymer photovoltaic solar cells (PVCs) have been attracting steady attention due to their potential application for large area, flexible, and low-cost solar cells, in the last decades.[1,2] Tremendous efforts such as the development of novel low band gap (LBG) CPs,[3–16] the optimization of the fabricating process[17] and modifying the morphology of the donor and acceptor blend[18,19] *etc.*, have been devoted to improving the power conversion efficiencies (PCEs) of PVCs. The development of high performance donor–acceptor (D–A) type LBG CPs has been demonstrated to be the most vigorous approach towards achieving efficient PVCs, and many promising D–A type LBG CPs have been developed in the last decades.[3–16] Among them, the most attractive sample is benzo[1,2-*b*:4,5-*b*′]dithiophene (**BDT**)-based CP. Many promising D-A type **BDT**-based LBG CPs have been demonstrated, and PCEs of 5.63–9.3% have been achieved in the PVCs from the polymers in recent years.[20–30]

As a notable aromatic analogue of **BDT**, dithieno[2,3-*d*:2′,3′-*d*′]benzo[1,2-*b*:4,5-*b*′]dithiophene (**DTBDT**) not only shows similar HOMO level with **BDT**, but also holds larger coplanar core and extended conjugation length. It was believed to provide advantageous properties for **DTBDT**-based CPs such as enhanced charge-carrier mobility, decreased band gaps and facilitated exciton separation into free charge carriers in contrast to **BDT**-based CPs.[31] Motivated by the attractive properties of **DTBDTs**-based CPs, many high performance **DTBDTs**-based CPs have been presented since Hou *et al.* firstly introduced the 5,10-di(2-hexyldecyloxy)-**DTBDT** to build the D–A type LBG CPs in 2012.[32] For instance, Yu *et al.* presented a series of LBG CPs based on 5,10-dialkyl-**DTBDT** and alkyl 3-fluorothieno-[3,4-*b*]thiophene-2-carboxylate in 2013.[33] Lately, Hou *et al.* presented CPs derived from 5,10-di(alkylthieno-2-yl)-**DTBDT** and 2-(2-hexyldecyl) sulfonylthieno[3,4-*b*]thiophene,[34] and Kwon *et al.* presented CPs derived from 5,10-di(alkylthieno-2-yl)-**DTBDT** and benzo-2,1,3-thiadiazole.[35] More recently, we have provided an effective approach to tune the optoelectronic properties of **DTBDTs**-based CPs *via* the changing of substituent groups on the **DTBDT**, and series of D–A type LBG CPs derived from **DTBDTs** and 3,6-bis(thieno-2-yl)-*N*,*N*′-dialkyl-1,4-dioxopyrrolo-[3,4-*c*]pyrrole.[36] In spite that PVCs from the D–A type LBG CPs derived from **DTBDTs** as electron donor units, have shown reasonably high PCEs of 3.5–7.6% to date,[32–36] the tailoring and enriching the family of the **DTBDTs**-based D–A type LBG CPs are still promising in the development of new ideal **DTBDTs**-based CPs for high performance PVCs.

In this paper, a low band gap conjugated polymer with 5,10-bis(4,5-didecylthieno-2-yl)-flanked-**DTBDT** as electron donor moieties and 4,9-bis(4-hexylthieno-2-yl)naphtho[1,2-*c*:5,6-*c*]bis-[1,2,5]-thiadiazole (**DTNT**) as electron acceptor moieties was synthesized through the palladium-catalyzed Stille coupling reaction under mono-microwave heating condition, and named as **PDTBDT-DTNT**. The **PDTBDT-DTNT** exhibited good solution processability and extensive absorption from 300 nm to 800 nm. The highest occupied molecular orbital (HOMO) and lowest unoccupied molecular orbital (LUMO) energy levels of the

[a]*Key Lab of Optoelectronic Technology and Intelligent Control of Education Ministry, Lanzhou Jiaotong University, Lanzhou, Gansu Province, 730070, China. E-mail: yjxia73@126.com; Fax: +86-093-1485-6058; Tel: +86-039-1495-6022*

[b]*Institute of Polymer Optoelectronic Materials and Devices, State Key Laboratory of Luminescent Materials and Devices, South China University of Technology, Guangzhou 510640, China. E-mail: msfhuang@scut.edu.cn; Fax: +86-020-8711-0606; Tel: +86-020-8711-4346*

[c]*College of Chemical and Biological Engineering, Lanzhou Jiaotong University, Lanzhou 730070, China*

† Electronic supplementary information (ESI) available. See DOI: 10.1039/c4ra14532a

PDTBDT-DTNT determined by cyclic voltammetry (CV) were about −5.51 eV and −3.90 eV, respectively. The photovoltaic property of **PDTBDT-DTNT** was also investigated, and the PCEs of 6.28% and 7.52% has been achieved in the traditional (with device configuration as: ITO/PEDOT:PSS/active layer/Ca/Al) and inverted (with device configuration as: ITO/poly[(9,9-bis(30-(*N*,*N*-dimethylamino)propyl)-2,7-fluorene)-*alt*-2,7-(9,9-ioctylfluorene)]/active layer/MoO_3/Ag) PVCs from the blend of **PDTBDT-DTNT** and [6,6]-phenyl-C_{71}-butyric acid methyl ester ($PC_{71}BM$) with weight ratio of 1 : 1 under AM 1.5 simulator (100 mW cm^{-2}), respectively.

Results and discussion

Synthesis and characterization of the PDTBDT-DTNT

The general synthetic route toward polymer is outlined in Scheme 1. 2,7-Bis(trimethylstannyl)-5,10-di(4,5-didecylthieno-2-yl)-**DTBDT** (**I**)[36] and 4,9-bis(5-bromo-4-hexylthieno-2-yl)naphtho[1,2-*c*:5,6-*c*]bis[1,2,5]thiadiazole (**BrDTNT**)[25] were synthesized as the procedure reported in the references. The structures of the monomers were confirmed by ^{1}H NMR and elemental analyses before use. The **PDTBDT-DTNT** was synthesized with **I** and **BrDTNT** through the palladium-catalyzed Stille coupling reaction under mono-microwave heating condition. Subsequently, the polymer was end-capped with 2-tributylstannylthiophene and 2-bromo-thiophene to remove bromo and trimethystannyl end groups. The ^{1}H NMR (400 MHz, $CDCl_3$) spectrum of the copolymer exhibited broad NMR signals at *ca.* 8.87, 8.17, 7.25–7.15, 3.08–2.97, and 2.30–0.90 ppm (Fig. 1). The 8.87 and 8.17 ppm correspond to the aromatic H atoms of **DTNT** rings in the copolymer backbone, and 7.25–7.15 ppm correspond to the aromatic H atoms on the **I** rings in the copolymer backbone. We also monitored the ^{1}H NMR signal at 3.08–2.97 ppm belonging to the α-H atoms of alkyl on **I** and **DTNT**. ^{1}H NMR spectrum of the copolymer confirmed that the copolymer is right on target alternating molecular structures containing 5,10-di(4,5-didecylthieno-2-yl)dithieno[2,3-*d*:2′,3′-*d*′]benzo[1,2-*b*:4,5-*b*′]dithiophene and 4,9-bis(4-hexylthieno-2-yl)naphtho[1,2-*c*:5,6-*c*]-bis-[1,2,5]thiadiazole. The number-average molecular weight of the **PDTBDT-DTNT** determined by GPC in tetrahydrofuran (THF) with polystyrene standards, is about $M_n = 26\,400$ g mol^{-1} with PDI of 2.35. The decomposed temperature (T_d, 5% weight-loss) of the **PDTBDT-DTNT** is about 423.6 °C (see ESI, SFig. 1†).

Optical and electrochemical property of PDTBDT-DTNT

The UV-vis absorption spectra of **PDTBDT-DTNT** in chloroform solution and solid thin film were monitored on a UV-2550 spectrophotometer, and presented in Fig. 2a. As shown in Fig. 2a, the **PDTBDT-DTNT** exhibits three absorption peaks at 350 nm, 493 nm and 733 nm with two shoulder absorption peaks at around 466 nm and 670 nm in chloroform solution. The **PDTBDT-DTNT** in solid thin film shows similar absorption spectrum except that the absorption peak at around 350 nm is decreased and the absorption peak at around 493 nm is increased in contrast to those for the absorption of **PDTBDT-DTNT** in solution. The optical band gap (E_g) of **PDTBDT-DTNT** estimated from the onset of absorption edge in solid thin film is about 1.58 eV (Fig. 2a).

The electrochemical behaviour of the polymer film was investigated by cyclic voltammetry in a nitrogen-saturated solution of 0.1 M tetrabutylammonium hexafluorophosphate in acetonitrile with glass carbon and $Ag/AgNO_3$ electrode as the working and reference electrode, respectively. All scans were performed at a scan rate of 0.1 V s^{-1}. The oxidation potential of **PDTBDT-DTNT** was observed at around 0.50 eV, and the reduction potential was observed at around −1.12 eV (Fig. 2b). The $E_{1/2}$ of ferrocene/ferrocenium (Fc/Fc^+) was observed at 0.09 V *vs.* Ag/Ag^+. The HOMO and LUMO energy levels were estimated from the onset of the oxidation and reduction waves, respectively, and the value of 5.1 eV *vs.* vacuum was used for Fc/Fc^+,[37] *i.e.*, HOMO $= -[E_{onset,ox} - 0.09 + 5.1]$ eV and LUMO $= -[E_{onset,red} - 0.09 + 5.1]$ eV. Thus, the HOMO and LUMO levels were −5.51 eV and −3.9 eV, respectively. The electrochemical gap (1.61 eV) is slightly higher than the optical one (1.58 eV) which was determined from the onset band gap wavelength of **PDTBDT-DTNT** in thin film. A comparison between the two gaps not only provides further support to the validity of considering the redox potentials and absorption maxima for a correct evaluation of energy gaps, but also gets involved in the exciton binding energy of conjugated polymers.[38,39]

Charge transporting property of PDTBDT-DTNT

To investigate the influence of the extended coplanar core and conjugation length of the 5,10-di(4,5-didecylthieno-2-yl)-**DTBDT** units on the hole mobility of **PDTBDT-DTNT**, the hole mobility of **PDTBDT-DTNT** was determined by applying the space-charge

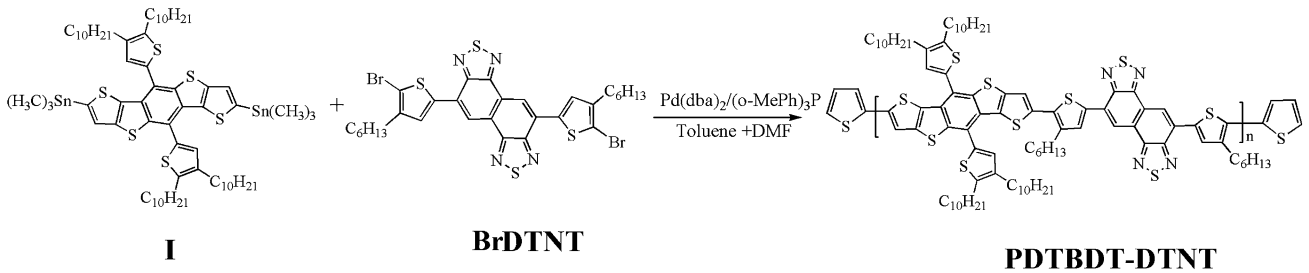

Scheme 1 Synthetic route of PDTBDT-DTNT.

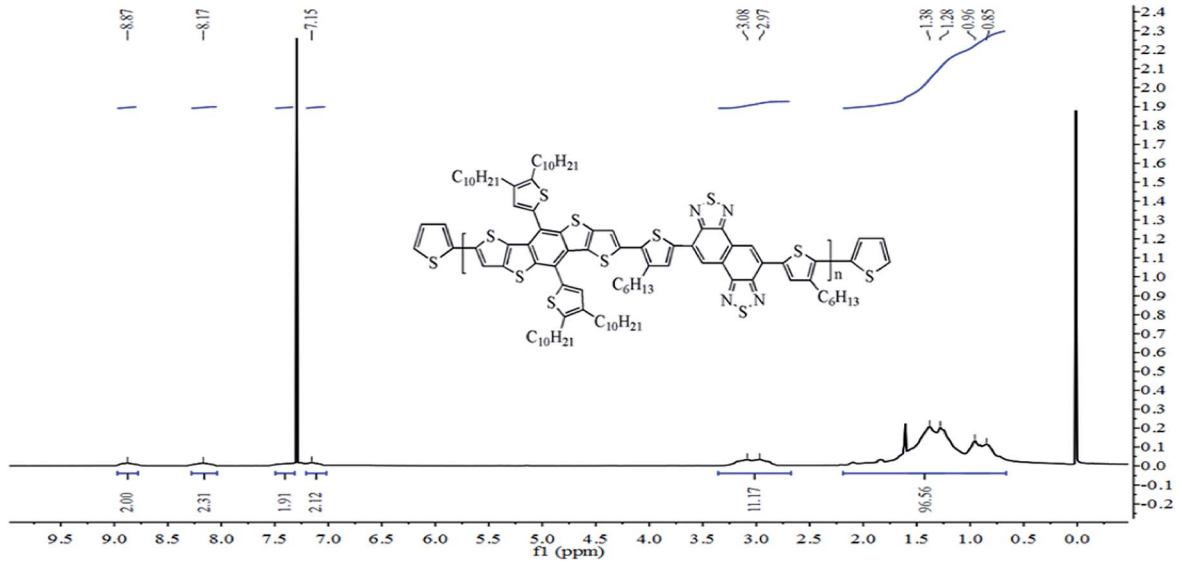

Fig. 1 ^{1}H NMR spectra of **PDTBDT-DTNT** in $CDCl_3$.

limited current (SCLC) model.[28] The hole mobility was found to be 8.28×10^{-5} cm^2 V^{-1} s^{-1} for **PDTBDT-DTNT** in comparison to 3.0×10^{-5} cm^2 V^{-1} s^{-1} for **PBDT-DTNT** Fig. 3.[25] Because the **PDTBDT-DTNT** hold similar molecular weight and side alkyl chains as compared with the **PBDT-DTNT** derived from 4,8-di(4,5-didecylthieno-2-yl)-**BDT** and **DTNT**, except that the coplanar core and conjugation length of 5,10-di(4,5-didecylthieno-2-yl)-**DTBDT** is larger than that for 4,8-di(4,5-didecylthieno-2-yl)-**BDT**. The higher hole mobility of **PDTBDT-DTNT** probably contributes the larger coplanar core area and extended conjugation of 5,10-di(4,5-didecylthieno-2-yl)-**DTBDT**.

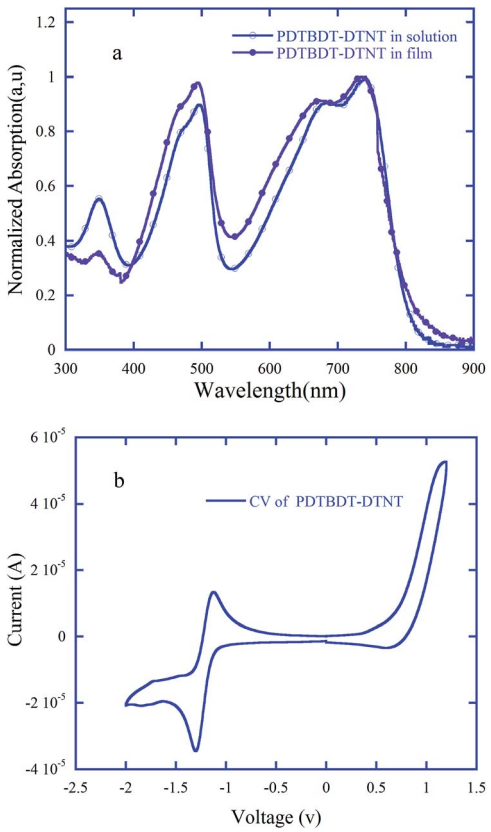

Fig. 2 Normalized absorption spectra of **PDTBDT-DTNT** in chloroform solution and solid thin film (a), electrochemical property of **PDTBDT-DTNT** (b).

Photovoltaic property of PDTBDT-DTNT

The **PDTBDT-DTNT**, as the electron donor materials for PVCs, was employed in PVCs with device configuration of ITO/PEDOT:PSS/active layer/Ca/Al (traditional PVCs), and $PC_{71}BM$ as the electron acceptor materials. The weight ratios of **PDTBDT-DTNT** and $PC_{71}BM$ were varied from 1 : 1 to 1 : 1.5 and then up to 1 : 2. The devices were characterized under AM 1.5 simulator (100 mW cm^{-2}). The PCEs of the traditional PVCs were varied from 5.30% to 4.13% and dropped to 3.16% with the open circuit voltage of 0.70 V, short current densities ranging from 10.33–14.50 mA cm^{-2} and fill factor ranging from 43.68–52.50% (Table 1, see ESI, SFig2†), while the weight ratios of

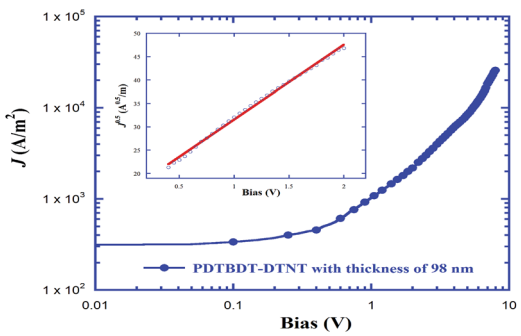

Fig. 3 *I*–*V* characteristics of the SCLC measurement of **PDTBDT-DTNT**.

Table 1 Photovoltaic parameters of PVCs from **PDTBDT-DTNT**/$PC_{71}BM$

Device configuration	Active layer	DIO (%)	V_{oc} (V)	J_{sc} (mA cm^{-2})	J_{cal} (mA cm^{-2})	FF (%)	η (%)
Traditional PVCs	**PDTBDT-DTNT**/$PC_{71}BM$ (1 : 1)	0	0.70	14.50	14.18	52.50	5.30
Traditional PVCs	**PDTBDT-DTNT**/$PC_{71}BM$ (1 : 1.5)	0	0.70	11.43	—	51.63	4.13
Traditional PVCs	**PDTBDT-DTNT**/$PC_{71}BM$ (1 : 2)	0	0.70	10.33	—	43.68	3.16
Traditional PVCs	**PDTBDT-DTNT**/$PC_{71}BM$ (1 : 1)	3	0.70	14.98	15.16	60.0	6.28
Inverted PVCs	**PDTBDT-DTNT**/$PC_{71}BM$ (1 : 1)	3	0.65	17.51	17.08	66.0	7.52

PDTBDT-DTNT and PC71BM were varied from 1 : 1 to 1 : 1.5 and then up to 1 : 2. It could be found that the optimal weight ratio of **PDTBDT-DTNT** and PC71BM was 1 : 1.

To modify the PVCs from **PDTBDT-DTNT**, the optimization of the morphologies of the blend films from **PDTBDT-DTNT**/$PC_{71}BM$ *via* the induction of 1,8-diiodooctane (DIO) in the fabrication of the devices were implemented, and the weight ratio of **PDTBDT-DTNT** and $PC_{71}BM$ was fixed at 1 : 1. Similar to the results in the reported works,[40,41] the PCEs of PVCs from **PDTBDT-DTNT**/$PC_{71}BM$ was clearly increased while 3% (V_{DIO} : $V_{chlorobenzene}$, 3 : 100) of DIO was added to the solution of **PDTBDT-DTNT**/$PC_{71}BM$ (w/w, 1 : 1) in chlorobenzene solution. And PVCs with PCEs of 6.28%, V_{oc} of 0.70 V, J_{sc} of 14.98 mA cm^{-2} and FF of 60.0% were achieved (Table 1, Fig. 4a). The results from AFM and TEM measurements of blend films of **PDTBDT-DTNT**/$PC_{71}BM$ (w/w, 1 : 1) indicated that the using of DIO could induce rougher surface and larger D–A interfaces of the films of **PDTBDT-DTNT**/$PC_{71}BM$ (see ESI, SFig. 3 and SFig. 4†),[42] thus lead much higher J_{sc} and FF and enhance the PCEs of the corresponding PVCs. According to the incident-photo-to-converted current efficiency (IPCE) curves (Fig. 4b), the integral current density values (J_{cal}, Table 1) of the devices are 14.18 mA cm^{-2}, 15.16 mA cm^{-2} and 17.08 mA cm^{-2}, respectively. The deviations between the integral current density and the J_{ac} read from the *J–V* measurement are within 3%, indicting the consistency of photovoltaic results.

In recently, it has been demonstrated that the inverted PVCs may take advantages such as the vertical phase separation, reduction of bimolecular recombination, and enhancement of absorption of photons *etc.*, thus to improve the J_{sc} and FF of the inverted PVCs.[24] To further modify the PVCs from **PDTBDT-DTNT**/$PC_{71}BM$, the inverted PVCs with the devices configuration as ITO/PFN/**PDTBDT-DTNT**/$PC_{71}BM$ (w/w, 1 : 1)/MoO_3/Ag were also fabricated and characterized. As shown in Fig. 4a and Table 1, the V_{oc} of the inverted PVCs were slightly decreased in contrast to that for the traditional PVCs (0.70 V *vs.* 0.65 V), and the J_{sc} and FF of the inverted PVCs were increased about 16.9% and 10% (17.51 mA cm^{-2} *vs.* 14.98 mA cm^{-2}, 66.0% *vs.* 60.0%) in contrast to those for traditional PVCs. As the inverted structure harvested more photons from solar spectra than the traditional PVCs (Fig. 5a), calculated by One Dimensional

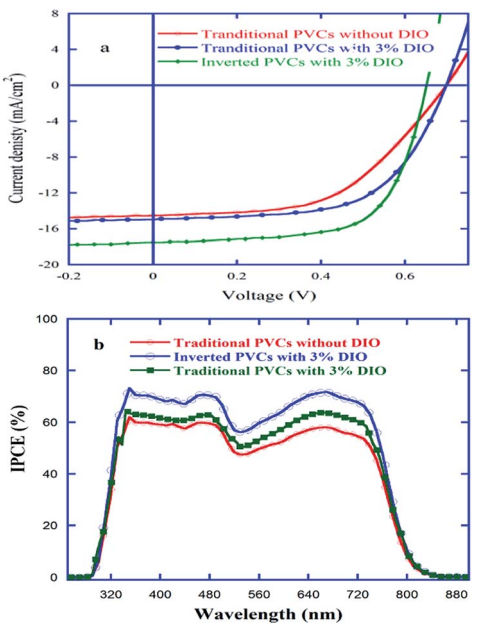

Fig. 4 *J–V* (a) and IPCEs (b) curves of PVCs from the blend of **PDTBDT-DTNT** and $PC_{71}BM$ with weight ratio of 1 : 1.

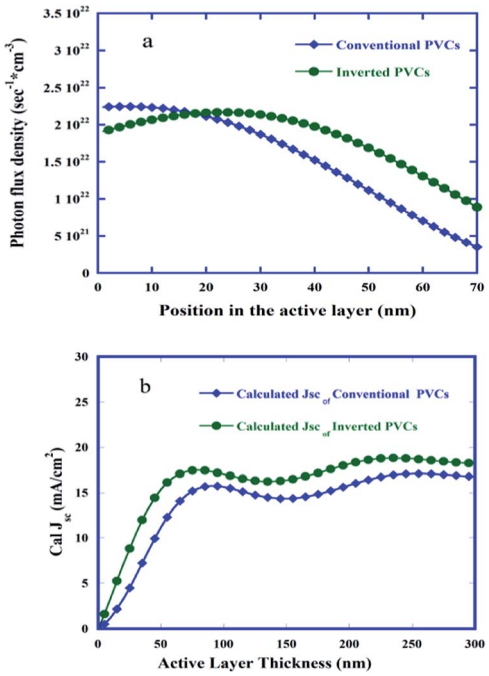

Fig. 5 Distribution of absorbed AM 1.5 G photon flux density inside the active layer (a) and the calculated J_{sc} of conventional and inverted PVCs from **PDTBDT-DTNT**/$PC_{71}BM$ (w/w, 1 : 1) with assuming average IQE of 85% (b).

Transfer Matrix Formalism (TMF),[24,43,44] and the calculated J_{sc} of the inverted PVCs was increased about 10% as compared with those for traditional PVCs (Fig. 5b), the enhancement of the J_{sc} for the inverted PVCs should mainly be attributed to the increase of the more photons from solar spectra in contrast to the traditional PVCs. On the other hand, although we did not achieved to monitor the desirable vertical phase separation like of the relative enrichment of the acceptor materials ($PC_{71}BM$) at bottom surfaces and the reduction of acceptor materials (**PDTBDT-DTNT**) at the top interfaces of the inverted PVCs at this stage, the enhancement of the FF and the remaining part of the increase of J_{sc} for the inverted PVCs might be attributed to the exhibiting favourable vertical phase separation of the inverted PVCs.

Conclusions

In this paper, a low band gap conjugated polymer with 5,10-bis(4,5-didecylthieno-2-yl)-flanked-**DTBDT** as electron donor units and 4,9-bis(4-hexylthieno-2-yl)naphtho[1,2-*c*:5,6-*c*]bis-[1,2,5]thiadia-zole (**DTNT**) as electron acceptor units, was synthesized through the palladium-catalyzed Stille coupling reaction under mono-microwave heating condition, and named as **PDTBDT-DTNT**. The chemical structure, molecular weight and optoelectronic properties *etc.* of **PDTBDT-DTNT** were characterized by gel permeation chromatography (GPC), ^{1}H NMR, UV-vis absorption spectra and cyclic voltammetry (CV) *etc.* The photovoltaic property of **PDTBDT-DTNT** was also investigated, and the PCEs of 6.28% and 7.52% has been achieved in the traditional and inverted PVCs from the blend of **PDTBDT-DTNT** and [6,6]-phenyl-C_{71}-butyric acid methyl ester ($PC_{71}BM$) with weight ratio of 1 : 1 under AM 1.5 simulator (100 mW cm^{-2}), respectively.

Experimental section

Materials

All reagents, unless otherwise specified, were obtained from Aldrich, Acros and TCI Chemical Co., and used as received. All the solvents were further purified under a nitrogen flow. 2,7-Bis(trimethylstannyl)-5,10-di(4,5-didecylthien-2-yl)dithieno[2,3-*d*:2′,3′-*d*′]benzo[1,2-*b*:4,5-*b*′]dithiophene (**I**)[36] and 4,9-bis(5-bromo-4-hexylthieno-2-yl)naphtho[1,2-*c*:5,6-*c*]bis[1,2,5]thiadiazole (**BrDTNT**)[25] were synthesized as the procedures reported in references, and characterized by ^{1}H NMR and FAB-MS before use. Poly[(9,9-bis(30-(*N*,*N*-dimethylamino)propyl)-2,7-fluorene)-*alt*-2,7-(9,9-dioctylfluorene)] (PFN)[40] were prepared and characterized by the procedure as reported reference.

General methods

^{1}H NMR spectra were recorded on a Breuker DRX 400 spectrometer operating at 400 MHz and were referred to tetramethylsilane. FAB-MS were obtained on VG ZAB-HS. The polymerization reactions were carried on a mono-microwave system (NOVA, PreeKem Scientific Instruments Co.) Analytical GPC was performed using a Waters GPC 2410 in tetrahydrofuran (THF) relative to polystyrene standards. Elemental analyses were performed on a Vario EL Elemental Analysis Instrument (Elementar Co.) Thermal gravimetric analysis (TGA) was conducted on a TGA 2050 (TA instruments) thermal analysis system under a heating rate of 10 °C min^{-1} and a nitrogen flow rate of 20 mL min^{-1}. UV-visible absorption spectra were measured on a UV-2550 spectrophotometer (Shimadzu Co.). The cyclic voltammetry (CV) of the **PDTBDT-DTNT** was measured on CHI 660 electrochemical workstation (Shanghai Chenhua Co.) at a scan rate of 50 mV s^{-1} with a nitrogen-saturated solution of 0.1 M tetrabutylammonium hexafluorophosphate (Bu_4NPF_6) in acetonitrile (CH_3CN) with glass carbon and $Ag/AgNO_3$ electrode as the working and reference electrode, respectively. Tapping-mode atomic force microscopy (AFM) images were obtained using a NanoScope NS3A system (Digital Instrument). Transmission electron microscopy (TEM) images were obtained using JEM-2100F FIELD EMISSION ELECTRON MICROSCOPE (JEOL).

Preparation and characterization of the photovoltaic solar cells

A patterned indium tin oxide (ITO) coated glass with a sheet resistance of 10–15 Ω per sq^{-1} was cleaned by a surfactant scrub, followed by a wet-cleaning process inside an ultrasonic bath, beginning with de-ionized water, followed by acetone and iso-propanol. After oxygen plasma cleaning for 5 min, a 40 nm thick poly(3,4-ethylenedioxythiophene):poly(styrene sulfonate) (PEDOT:PSS) (Bayer Baytron 4083) anode buffer layer was spin-casted onto the ITO substrate and then dried by baking in a vacuum oven at 80 °C overnight. The active layer, with a thickness in the 70–80 nm range, was then deposited on top of the PEDOT:PSS layer by spin-casting from the chlorobenzene solution containing **PDTBDT-DTNT**/$PC_{71}BM$ (w/w, 1 : 1, 1 : 1.5 and 1 : 2) with and without DIO. Then a 8 nm calcium and a 100 nm aluminium layer were evaporated with a shadow mask under vacuum of (1–5) × 10^{-5} Pa. The overlapping area between the cathode and anode defined a pixel size of device of 0.1 cm^2. The thickness of the evaporated cathode was monitored by a quartz crystal thickness/ratio monitor (SI-TM206, Shenyang Sciens Co.). Except for the deposition of the PEDOT:PSS layers, all the fabrication processes were carried out inside a controlled atmosphere in a nitrogen drybox (Etelux Co.) containing less than 1 ppm oxygen and moisture. The power conversion efficiencies (PCEs) of the resulting polymer solar cells were measured under 1 sun, AM 1.5 G (Air mass 1.5 global) condition using a solar simulator (XES-70S1, San-EI Electric Co.) with irradiation of 100 mW cm^{-2}. The current density–voltage (*J*–*V*) characteristics were recorded with a Keithley 2400 source-measurement unit. The spectral responses of the devices were measured with a commercial EQE/incident photon to charge carrier efficiency (IPCE) setup (7-SCSpecIII, Bejing 7-star Opt. In. Co.). A calibrated silicon detector was used to determine the absolute photosensitivity.

Synthesis of PDTBDT-DTNT

A mixture of toluene (6 mL) and *N*,*N*-dimethylformamide (DMF, 0.5 mL) was added to a 55 mL microwave tube containing 2,7-bis(trimethylstannyl)-5,10-di(4,5-didecylthien-2-yl)dithieno-[2,3-*d*:2′,3′-*d*′]benzo[1,2-*b*:4,5-*b*′]dithiophene (271.1 mg, 0.2 mmol), 4,9-bis(2-bromo-4-hexylthieno-2-yl)naphtho[1,2-*c*:5,6-*c*]-bis[1,2,5]thiadiazole (146.9 mg, 0.2 mmol), $Pd(dba)_2$ (2.0 mg) and tris(3-methoxyphenyl)phosphine (4 mg) in a glove box with moisture and oxygen under 1 ppm. Then the tube was subjected to the following reaction conditions in a mono-microwave reactor: 120 °C for 5 min, 140 °C for 5 min and 160 °C for 20 min. At the end of polymerization, the polymer was end-capped with 2-tributylstannylthiophene and 2-bromo-thiophene to remove bromo and trimethystannyl end groups. The mixture was then poured into methanol. The precipitated material was collected and extracted with ethanol, acetone, hexane and toluene in a Soxhlet extractor. The solution of the copolymer in toluene was condensed to 20 mL and then poured into methanol (500 mL). The precipitation was collected and dried under vacuum overnight (yield: 75%). M_n = 26 400 g mol^{-1} with a polydisperse index (PDI) of 2.35. ^1H NMR ($CDCl_3$, 400 MHz), 8.87, 8.17, 7.25–7.15, 3.08–2.97, and 2.30–0.90 ppm.

Acknowledgements

This work is financially supported the Ministry of Science and Technology (no. 2014CB643501), National Science Foundation of China (61166002, 21125419 61264002, 91333206, 51463011), Gansu Province Natural Foundation (#1107RJZA154, 1111RJDA009, 1308RJZA159) and the Program for New Century Excellent Talents in University of Ministry of Education of China (Grant no. NCET-13-0840).

Notes and references

1 N. S. Sariciftci, L. Smilowitz, A. J. Heeger and F. Wudl, *Science*, 1992, **258**, 1474–1476.
2 G. Yu, J. Gao, J. C. Hummelen, F. Wudl and A. J. Heeger, *Science*, 1995, **270**, 1789–1791.
3 T. Kietzke, H.-H. Hörhold and D. Nehe, *Chem. Mater.*, 2005, **17**, 6532–6537.
4 M. M. Wienk, J. M. Kroon, W. J. H. Verhees, J. Knol, J. C. Hummelen, P. A. van Hal and R. A. J. Janssen, *Angew. Chem., Int. Ed.*, 2003, **42**, 3371–3375.
5 Q. Zhou, Q. Hou, L. Zheng, X. Deng, G. Yu and Y. Cao, *Appl. Phys. Lett.*, 2004, **84**, 1653–1655.
6 L. Liu, C.-L. Ho, W.-Y. Wong, K.-Y. Cheung, M.-K. Fung, W.-T. Lam, A. B. Djurišić and W.-K. Chan, *Adv. Funct. Mater.*, 2008, **18**, 2824–2833.
7 M.-H. Chen, J. Hou, Z. Hong, G. Yang, S. Sista, L.-M. Chen and Y. Yang, *Adv. Mater.*, 2009, **21**, 4238–4242.
8 F. Huang, K.-S. Chen, H.-L. Yip, S. K. Hau, O. Acton, Y. Zhang, J. Luo and A. K.-Y. Jen, *J. Am. Chem. Soc.*, 2009, **131**, 13886–13887.
9 N. Blouin, A. Michaud and M. Leclerc, *Adv. Mater.*, 2007, **19**, 2295–2300.
10 E. Wang, L. Wang, L. Lan, C. Luo, W. Zhuang, J. Peng and Y. Cao, *Appl. Phys. Lett.*, 2008, **92**, 033307.
11 C. Duan, W. Cai, F. Huang, J. Zhang, M. Wang, T. Yang, C. Zhong, X. Gong and Y. Cao, *Macromolecules*, 2010, **43**, 5262–5268.
12 W. Y. Wong, X. Z. Wang, Z. He, A. B. DjuriŠiĆ, C. T. Yip, K. Y. Cheung, H. Wang, C. S. K. Mak and W. K. Chan, *Nat. Mater.*, 2007, **6**, 521–527.
13 R. C. Coffin, J. Peet, J. Rogers and G. C. Bazan, *Nat. Chem.*, 2009, **1**, 657–661.
14 Y. Xia, Y. Li, Y. Zhu, J. Li, P. Zhang, J. Tong, C. Yang, H. Li and D. Fan, *J. Mater. Chem. C*, 2014, **2**, 1601–1604.
15 Y. Xia, Y. Gao, Y. Zhang, J. Tong, J. Li, H. Li, D. Chen and D. Fan, *Polymer*, 2013, **54**, 607–613.
16 Z. Ma, D. Dang, Z. Tang, D. Gedfaw, J. Bergqvist, W. Zhu, W. Mammo, M. R. Andersson, O. Inganas, F. Zhang and E. Wang, *Adv. Energy Mater.*, 2014, **4**, 1301455.
17 J. Peet, M. L. Senatore, A. J. Heeger and G. C. Banzan, *Adv. Mater.*, 2009, **21**, 1521–1527.
18 J. Peet, J. Y. Kim, N. E. Coates, W. L. Ma, D. Mose, A. J. Heeger and G. C. Banzan, *Nat. Mater.*, 2007, **6**, 497–500.
19 L. Ye, S. Zhang, W. Ma, B. Fan, X. Guo, Y. Huang, H. Ade and J. Hou, *Adv. Mater.*, 2012, **24**, 6335–6341.
20 T.-Y. Chu, J. Lu, S. Beaupré, Y. Zhang, J.-R. Pouliot, S. Wakim, J. Zhou, M. Leclerc, Z. Li, J. Ding and Y. Tao, *J. Am. Chem. Soc.*, 2011, **133**, 4250–4253.
21 J. Hou, H.-Y. Chen, S. Zhang, G. Li and Y. Yang, *J. Am. Chem. Soc.*, 2008, **130**, 16144–16145.
22 Y. Liang, D. Feng, Y. Wu, S.-T. Tsai, G. Li, C. Ray and L. Yu, *J. Am. Chem. Soc.*, 2009, **131**, 7792–7799.
23 Y. Liang, Z. Xu, J. Xia, S.-T. Tsai, Y. Wu, G. Li, C. Ray and L. Yu, *Adv. Mater.*, 2010, **22**, E135–E138.
24 Z. He, C. Zhong, S. Su, M. Xu, H. Wu and Y. Cao, *Nat. Photonics*, 2012, **6**, 591–595.
25 M. Wang, X. Hu, P. Liu, W. Li, X. Gong, F. Huang and Y. Cao, *J. Am. Chem. Soc.*, 2011, **133**, 9638–9641.
26 T. Yang, M. Wang, C. Duan, X. Hu, L. Huang, J. Peng, F. Huang and X. Gong, *Energy Environ. Sci.*, 2012, **5**, 8208–8214.
27 L. Huo, S. Zhang, X. Guo, F. Xu, Y. Li and J. Hou, *Angew. Chem.*, 2011, **123**, 9871–9876.
28 L. Dou, J. You, J. Yang, C.-C. Chen, Y. He, S. Murase, T. Moriarty, K. Emery, G. Li and Y. Yang, *Nat. Photonics*, 2012, **6**, 180–185.
29 Y. Huang, X. Guo, F. Liu, L. Huo, Y. Chen, T. P. Russel, C. C. Han, Y. Li and J. Hou, *Adv. Mater.*, 2012, **24**, 3383–3389.
30 Z. Ma, E. Wang, M. E. Jarvid, P. Henriksson, O. Inganäs, F. Zhang and M. R. Andersson, *J. Mater. Chem.*, 2012, **22**, 2306–2314.
31 P. Gao, D. Beckmann, H. N. Tsao, X. Feng, V. Enkelmann, M. Baumgarten, W. Pisula and K. Müllen, *Adv. Mater.*, 2009, **21**, 213–216.
32 Y. Wu, Z. Li, X. Guo, H. Fan, L. Huo and J. Hou, *J. Mater. Chem.*, 2012, **22**, 21362–21365.
33 H. J. Son, L. Lu, W. Chen, T. Xu, T. Zheng, B. Carsten, J. Strzalka, S. B. Darling, L. X. Chen and L. Yu, *Adv. Mater.*, 2013, **25**, 838–843.

34 Y. Wu, Z. Li, W. Ma, Y. Huang, L. Huo, X. Guo, M. Zhang, H. Ade and J. Hou, *Adv. Mater.*, 2013, **25**, 3449–3455.
35 H.-J. Yun, Y.-J. Lee, S.-J. Yoo, D. S. Chung, Y.-H. Kim and S.-K. Kwon, *Chem.–Eur. J.*, 2013, **19**, 13242–13248.
36 S. Shuo, P. Zhang, J. Li, J. Tong, J. Wang, S. Zhang, Y. Xia, X. Meng, D. Fan and J. Chu, *J. Mater. Chem. A*, 2014, **2**, 15316–15325.
37 C. M. Cardona, W. Li, A. E. Kaifer, D. Stockdale and G. C. Bazan, *Adv. Mater.*, 2011, **23**, 2367–2371.
38 Y. Zhu, R. D. Champion and S. A. Jenekhe, *Macromolecules*, 2006, **39**, 8712–8719.
39 N. S. Sariciftci, *Primary Photoexcitations in Conjugated Polymers: Molecular Excitons vs. Semiconductor Band Model*, World Scientific, Singapore, 1997.
40 J. Peet, J. Y. Kim, N. E. Coates, W. L. Ma, D. Mose, A. J. Heeger and G. C. Banzan, *Nat. Mater.*, 2007, **6**, 497–500.
41 A. K. K. Kyaw, D. H. Wang, C. Luo, Y. Cao, T.-Q. Nguyen, G. C. Bazan and A. J. Heeger, *Adv. Energy Mater.*, 2014, **4**, 1301469.
42 S. H. Park, A. Roy, S. Beaupré, S. Cho, N. Coates, J. S. Moon, D. Moses, M. Leclerc, K. Lee and A. J. Heeger, *Nat. Photonics*, 2009, **3**, 297–302.
43 Z. He, H. Wu and Y. Cao, *Adv. Mater.*, 2014, **26**, 1006–1024.
44 C. Liang, Y. Wang, D. Li, X. Li, F. Zhang and Z. He, *Sol. Energy Mater. Sol. Cells*, 2014, **127**, 67–86.